NeQuick: In-Depth Analysis and New Developments

Bidaine, B. [(1)], Prieto-Cerdeira, R. [(2)], Orus, R. [(2)]

[(1)]University of Liège - Geomatics
Allée du 6-Août, 17
B-4000 Liège (Belgium)
Email: B.Bidaine@ulg.ac.be

[(2)] European Space Agency (ESA), ESTEC, Wave Interaction and Propagation Section (TEC-EEP)
Keplerlaan 1, 2201AZ
Noordwijk ZH (The Netherlands)
Email: Roberto.Prieto.Cerdeira@esa.int, Raul.Orus.Perez@esa.int

ABSTRACT

An empirical model called NeQuick has been selected for the modelling and correction of the ionospheric delay contribution in GALILEO single frequency receivers. The current baseline version of NeQuick for GALILEO is the one available in the International Telecommunication Union – Radiocommunication Sector (ITU-R) since 2001. From that time, several improvements have been proposed leading to the need of a better understanding and comparison of these different versions and an analysis of the weaknesses. Better results have been obtained by means of simpler ionosonde and profile parameters calculations, different topside formulation and new data files.

The interest of a newer version of NeQuick including the above-mentioned modifications is highlighted as its error behaviour towards latitude shows a better agreement with reality. Those modifications should be coupled to a less simplistic topside formulation involving several layers with appropriate transitions such as the proposal introduced in this paper. The need of a different treatment regarding the daily effective use of the model for GALILEO single frequency algorithm compared to a physical use (that uses monthly median underlying data) is addressed.

For the analysis and comparison of the different variants of the model, a software tool with a Graphical User Interface was developed. Preliminary comparisons for the physical use between different versions and also between modelled and measured data are presented. Such comparisons should be extended in the future for the effective use of the model.
Finally, the structure and analysis of the mentioned issues and the results of the different comparisons are shown. Also solutions or potential paths to investigate solutions are proposed.

1. INTRODUCTION

The Earth's ionosphere is a region of weakly ionised gas or plasma lying between about 50 kilometers up to several thousand kilometres from Earth's surface [1]. The ionisation is mainly due to solar radiation. The ionosphere is composed by a number of regions produced by different type of solar radiation and with different effects on radiowave propagation. In order of increasing height, those regions are named: D, E, F (which at the same time is subdivided into F1 and F2 layers) and the protonosphere. The presence of the Earth's magnetic field produces some effects on the ionosphere such as the anisotropy of the index of refraction or the plasma fountain effect that give raise to the equatorial anomaly.

The ionosphere affects radiowave propagation in different ways such as refraction, absorption, Faraday rotation, group delay, time dispersion or scintillations. As the ionospheric effects are dispersive, they are usually grouped by frequency bands and by the kind of systems working on such bands. A good review on general radiowave propagation ionospheric effects is [2], effects on satellite systems are well covered in [3], and for effects on Global Navigation Satellite Systems (GNSS), references [4] and [5] present a good starting point.

For GNSS, which are typically working in L band, one of the most important ionospheric problem is the pseudorange error introduced by the group delay on navigation signals (which is identical but with opposite sign to the carrier phase advance). This delay, if not corrected, can induce ranging errors up to 50 meters in L1 (1575.42 MHz) for days with high levels of electron density and low elevation satellites. In order to quantify analytically the group delay, it is necessary to know the relation between the velocity of light and the actual velocity of propagation of the signal through the ionosphere. This relation is given by the refractive index, which, for the ionosphere, is expressed by the Appleton

formula (see [1]), and depends, among other things, on carrier frequency and electron density. At a first order approximation, the code delay can be expressed as follows (higher order terms usually account for less than 0.1 % of the delay):

$$\sigma_{iono} = \frac{40.3}{f^2} \cdot \int_{path} N \cdot dl = \frac{40.3}{f^2} \cdot sTEC \tag{1}$$

Where σ_{iono} is the group delay error [m], f is frequency [Hz], N is electron density [electrons.m^{-3}], $sTEC$ is slant Total Electron Content [electrons.m^{-2}], and *path* is the propagation path between receiver and satellite. As the ionospheric group delay error is dispersive, GNSS receivers working in two or more frequencies can eliminate such delay.

Total Electron Content (TEC) is an important parameter to characterize the ionosphere since many ionospheric propagation effects are related to it. TEC is defined as the number of electrons in a column of one square meter cross section along a path through the ionosphere and it is usually represented in TEC units (TECu), where 1 TECu is 10^{16} electrons.m^{-2}. For GNSS, satellite-to-receiver paths are usually slant or oblique (sTEC), although vertical TEC (vTEC) is also often used together with a mapping function to translate vertical to slant, for instance, the ionospheric information broadcast by Satellite Based Augmentation Systems (SBAS) is a grid of vTEC and receivers implement a mapping function depending on the zenith angle. The value of TEC depends on different factors such as time of the day, location, season, solar activity (which is related to the epoch within the solar cycle) or level of disturbance of the ionosphere, such as those due to geomagnetic storms.

For the prediction of ionospheric characteristics, different models exist: from complex theoretical models that attempt to solve principle equations governing the processes in the ionospheric plasma, such as TDIM and GTIM models; to parametric models, that represent the ionospheric spatial and temporal description by a number of parameters, for instance, SLIM or PIM models; or, empirical models that use a statistical description, based on measurements, of some ionospheric parameters plus some analytical or theoretical descriptions. Some examples of empirical models are Bent, IRI, Chiu or NeQuick. A good review on models is [6]. There are also some models that allow ingestion or assimilation of real-time measured data, improving the accuracy on ionospheric predictions.

For GNSS single frequency users, since the ionospheric group delay can lead to large positioning errors, a model that allows predicting the ionospheric group delay is desired. GPS uses the Klobuchar ionospheric algorithm based on the Bent model [7]. For GALILEO, an ionospheric empirical model called NeQuick has been selected for computing ionospheric group delay corrections within the ionospheric single frequency users algorithm [8].

2. NEQUICK MODEL

NeQuick is an empirical quick-run ionospheric model, suitable for trans-ionospheric applications, which generates electron density for given space, time and solar activity conditions from a minimum set of anchor points characteristics. For the single frequency receiver in GALILEO, using NeQuick together with integration methods along the satellite-to-receiver path allows calculating slant TEC between a given user location and the space vehicles in sight. The current GALILEO baseline version of NeQuick is the one available in the ITU-R recommendation P.531 since 2001 [9]. It consists of two major components: the bottom side based on a modified version of the DGR model which contains ITU-R coefficients for foF2 and M(3000)F2 and simplified models for foF1 and foE that take into account the solar zenith angle, season and solar activity, and the topside model for the height region above the F2-layer peak, represented by a semi-Epstein layer with a height dependent thickness parameter. Details on ITU-R version are included in Appendix 1.

NeQuick is available in ITU-R as Fortran77 code [10] and it is labelled in this paper as ITU-R version, as it was first described in [11]. The input arguments are *position* with height h, geographic latitude φ and longitude θ, *season* with month, *solar activity* with monthly smoothed value of the solar radio flux at a wavelength of 10.7cm (Φ_{12} or *F10.7*) and *time-of-day* with universal time *UT*. The basic parameters are then computed from these inputs and from CCIR maps (files CCIRxx.asc). They still correspond to the origin and constraint of the ionosphere on:

1. *solar activity* with Φ_{12} and converted to 12-month smoothed monthly solar R_{12} (see eq. (10)-(11) in Appendix 1).
2. and *geomagnetism* with Modified Dip latitude (MODIP or μ) obtained from magnetic dip, I, which is itself calculated from the geomagnetic, dipolar or dip latitude (λ) assuming a dipole approximation of the Earth's magnetic field:

$$\tan I = 2 \tan \lambda \tag{2}$$

In NeQuick, geomagnetic latitude is computed from from the International Geomagnetic Reference Field (IGRF) model for the Earth's magnetic field [12] as a 3rd order Lagrange interpolation on a grid (5° in latitude and 10° in longitude) of data stored in the file *diplats.asc*. As a matter of fact, strictly speaking, the coordinates derived from such a model are defined as Corrected Geomagnetic Coordinates (CGM) [13], compared to typical geomagnetic coordinates derived from a dipole approximation. When NeQuick calculates magnetic dip and MODIP using CGM coordinates instead of using geomagnetic coordinates, these parameters should be denominated as Corrected Magnetic Dip (*I'*) and Corrected Modified Dip Latitude (MODIP') respectively. This distinction is usually not found on NeQuick references.

Several developments have been proposed for NeQuick since the release of the ITU-R version, intending to improve the model, leading to the need of a better understanding and comparison of these different representations, and, an analysis of strengths and weaknesses. These developments are analysed in this paper and will be presented in the following sections.

3. NEQUICK ASSESSMENT

Existing developments

The latitudinal dependence of group delay error is linked to the use of the geographic latitude parameter with empirical coefficients which is used in different parts of the model.

1. A *variable*, the MODIP, is computed from latitude so that, in parallel with associated equations, functions and subroutines, it may allow to represent it in a simpler way (such as a new mapping grid from CGM coordinates to MODIP).
2. The *basic parameters*, consisting of the ionosonde parameters, are also based on files, and could be updated and built differently, for instance, using directly solar flux Φ_{12} instead of sunspot number.
3. The *intermediate parameters*, including the Epstein and *k* parameters, are indirectly concerned as their equations, functions and subroutines use the basic parameters.
4. Finally the *topside* formulation is undergoing current research because the most important problems are thought to come from its too high simplicity and because, up to now, less data, from topside sounders for instance, was available to compare the model with measurements [14].

Modifications corresponding to the abovementioned issues have already been already proposed but not taken into account for GALILEO purpose. Main developments before ITU-R version are, first, the original DGR approach (three Epstein layers for bottom side) and, then, its evolution (five semi-Epstein layers for bottom side). Those developments have not been implemented during this work but their formulation is included in Appendix 1.

In 2002 (see [15]), the definition for f_0F_1 was revisited so that simplifications were introduced for $h^{F1}{}_{\max}$ and the thickness parameters. Peak amplitudes were also modified. This new formulation, labelled in this paper as NeQuick developments (2002), avoids strange structures and strong gradients in the E and F_1 layers (the evolution of $B^{F1}{}_{\text{top}}$ is shown in Fig. 1 and Fig. 2).

Two improvements were presented in 2005. The first one, labelled as NeQuick developments (2005a) [16], introduces a unique formula for the topside *k* parameter in lieu of the previous two equations formulation. The second, labelled as NeQuick developments (2005b), constitutes a very deep revision and it is not yet published. As a consequence, the modifications were analysed by reverse engineering from source code provided by the authors [17]. The principal changes are related to the proposal of new input data files:

1. a MODIP file (*modip_9.asc*) instead of the dip latitude file (*diplats.asc*)
2. and simplified ITU-R maps (*CCsimXX.asc* replacing *ccirXX.asc*).

The latest correspond to spherical harmonics approximation which does not use geographic latitude anymore and replaces universal time by local time so that smaller scale structures which do not reflect a realistic monthly median ionosphere could be removed. The roles of $h^{F2}{}_{\max}$ and $M(3000)F_2$ have also been inverted since $h^{F2}{}_{\max}$ is now computed by means of a numerical map. A more detailed description of all the modifications can be found in [18].

All these proposals and developments have been implemented under this study and some of the consequences are presented in the section "Analysis tool and tests".

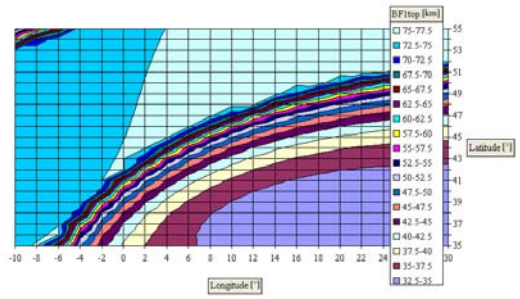

Fig. 1. $B^{F1}{}_{top}$ map from NeQuick ITU-R (November, Φ_{12}=100, 11h universal time)

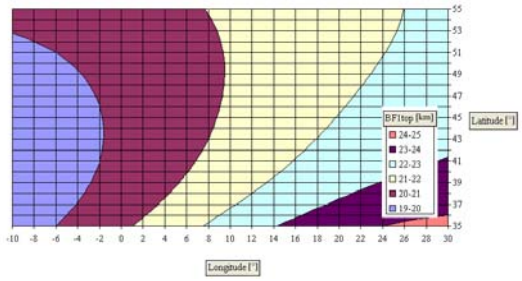

Fig. 2. $B^{F1}{}_{top}$ map from NeQuick developments (2002) (November, Φ_{12}=100, 11h universal time)

Future Developments

It is well known that most of the modelling errors come from the topside, so that attempts for new formulations are suitable. A simple evolution is proposed in this study by replacing the semi-Epstein profile from the ITU-R version (2001), first by a Chapman layer, labelled as NeQuick developments (2006a), and then by an hybrid layer involving a Chapman layer just above the F_2 peak changing fast into a modified Epstein layer, labelled as NeQuick developments (2006b).

The proposed ideas are based on [19], highlighting the need for new techniques to represent the transition between 0^+ and H^+ dominated ionosphere and of [14] advising a Chapman layer up to about 400km above F_2 layer peak.
As a consequence, a compromise is found by

- representing that transition (see Fig. 3) without new parameter by means of a Chapman and the original modified Epstein formulations – where the unknown thickness parameters as $B^{F2}{}_{top}$ for the Chapman layer and H for Epstein formulation are arbitrarily chosen;
- and, using an exponential transition to model the unknown transition height, which is undergoing current research.

The derived equations are shown below. and an example of resulting profile in given in Fig. 4:

$$N(h) = \frac{Ep(h)\exp\{50\,(Ch(h)-Ep(h))\}+Ch(h)}{\exp\{50\,(Ch(h)-Ep(h))\}+1}$$

$$Ch(h) = N_{\max}^{F_2}\exp\left\{0.5\left(1-\frac{h-h_{\max}^{F_2}}{B_{top}^{F_2}}-\exp\left(-\frac{h-h_{\max}^{F_2}}{B_{top}^{F_2}}\right)\right)\right\} \qquad (3)$$

$$Ep(h) = 4\,N_{\max}^{F_2}\frac{\exp\left(\frac{h-h_{\max}^{F_2}}{H}\right)}{\left(1+\exp\left(\frac{h-h_{\max}^{F_2}}{H}\right)\right)^2}$$

The hybrid formulation has been also combined with NeQuick developments (2005b) and they have been labelled here as NeQuick developments (2006).

Going then, towards the daily use (also designated in this paper as "effective" use) of NeQuick in the GALILEO single frequency algorithm (with respect to a "physical" use based on monthly median parameters), a new parameter called Effective Ionization Level, *Az,* which is calculated daily, replaces the Φ_{12} and the limit value of 193 for Φ_{12} is removed. One of the purposes of *Az* is to adapt potential TEC mismodelling in comparison with measured TEC. According to the monotonously increasing relationship with solar activity, Φ_{12} is replaced by *Az* resulting on lower values of f_0F_2. But at some point – when f_0F_2 reaches a value 0 –, decreasing *Az* further, does not decrease TEC anymore because of the second order relationship of the global electron density at the F_2 layer peak NmF_2 on f_0F_2 (see Appendix 1). Other means to decrease TEC further should be found elsewhere avoiding non-physical negative values of f_0F_2 (see Fig. 5).

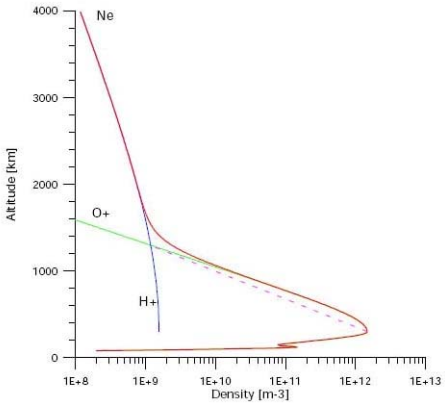

Fig. 3. Transition between 0^+ and H^+ dominated ionosphere (Source: [19])

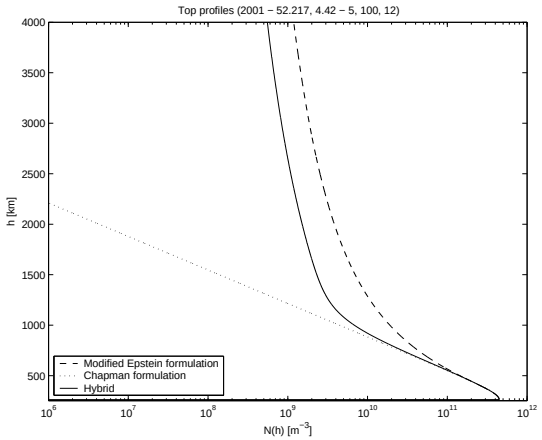

Fig. 4. Proposed topside formulations and NeQuick ITU-R version (ESTEC location – 52.217°N, 4.42°E –, May, average solar flux – Φ_{12}=100–, midday universal time)

A potential solution would be not considering NeQuick as a black box, but instead applying an intermediate approach for a daily use: apart from feeding NeQuick with the effective ionization level, *Az*, the use of daily values could lead to intrinsic modifications of the model (moving the "black box" to the CCIR files which will remain adapted for monthly values).

1. The characteristic levels of solar activity could be re-evaluated for the very first combination of coefficients from the CCIR maps, currently R_{12}=0 for low and R_{12}=100 for high. For example, a value of R*=200 could be chosen to represent high solar activity level (where R* would denote a daily effective sunspot number).
2. Consequently it would be necessary to build a new relationship between flux and sunspot number, linking *Az* to R*, or just use *Az* directly on all model calculations, instead of the sunspot number.

This broad analysis would not be complete without taking into account the questions related to the language used to implement the model and associated drivers and to the numerical tools chosen such as interpolation or integration methods. Beside the ITU-R code, a C++ source code version is also available, and it was developed for an improved performance daily use based on ITU-R version with the following modifications:

- the modifications leading to NeQuick developments (2002) were included ;
- a MODIP file has already been taken into account (*modip2001.asc*) instead of the diplats file ;
- the effective ionisation level *Az* is used as input parameter ;
- the integration routine has been modified for improved performance, although this is not part of the model itself but of the implementation. It is proposed to use Kronrod quadrature $G_7 - K_{15}$ [20] instead of the Gauss-Legendre quadrature integration available in the driver examples of the ITU-R source code, providing less function calls, decrease of average relative error and decrease of total computation time.

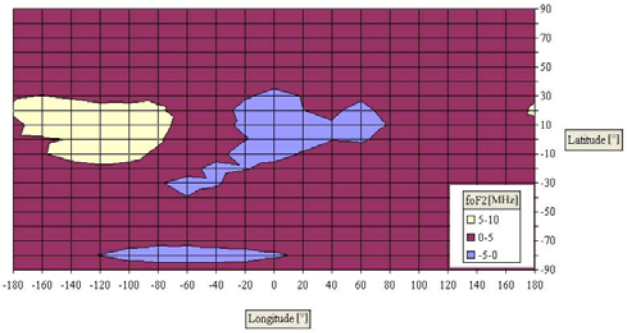

Fig. 5. f_0F_2 map for *Az*=10 (ESTEC location – 52.217°N, 4.42°E –, May, midnight universal time)

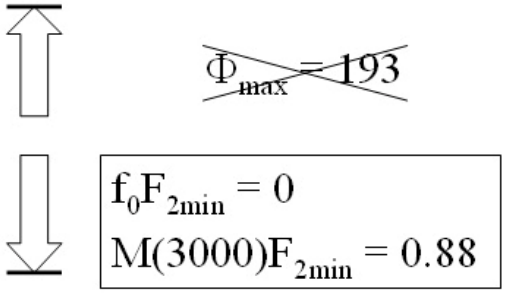

Fig. 6. New "effective" limits

4. ANALYSIS TOOL AND TESTS

In order to test the different evolutions of NeQuick in a more straightforward way and to easily visualize and store the results, a combination of FORTRAN programs and a Matlab Graphical User Interface were developed. Through this tool, it is possible to:

1. calculate electron densities for one or all mentioned versions and developments of NeQuick ;
2. plot electron density profiles for one or many versions, as well as the decomposition of the bottom side into its different layers, a comparison between different topside formulations or comparison between maximum five profiles for the same version ;
3. perform vertical TEC analysis by means of maps by comparing absolute and relative vTEC differences between different developments, as well as, global values or curves of bias, maximum and RMS of these differences ;
4. and perform slant TEC analysis by comparing modelled values of NeQuick and GPS data through global values or curves of bias, maximum and RMS of absolute and relative sTEC differences.

An auxiliary tool is also available to convert smoothed monthly sunspot numbers into corresponding fluxes or to look for past measured values of these parameters from the SIDC (Solar Index Data Center) in Brussels (http://sidc.oma.be/DATA/monthssn.dat).

Description of Tests

A number of tests have been performed with the analysis tool mentioned above. Table 1 specify the meaning of the different parameters that have been used for the comparisons, where <> denotes average, TEC_{ref} is the TEC reference value, in comparison with TEC_{mod} which is the modelled TEC value that is being compared.

A thorough study implies to take various conditions into account following the general ionospheric variations. The performed tests are described below.

Profile analysis: three latitudes – low (Dakar (DAKA): 14.68°N, −17.46°E), mid (ESTEC: 52.217°N, 4.42°E) and high (Ny-Alesund (NYAL): 78.9°N, 11.9°E); three seasons – winter (December), equinox (March) and summer (June); three solar activity levels – low (Φ_{12}=63), mid (Φ_{12}=123) and high (Φ_{12}=183); and several times-of-day paying attention to the different longitudes – approximately 0 and 12LT (UT: 0 and 12 for Dakar, 1 and 13 for ESTEC, 2 and 14 for Ny-Alesund).

vTEC analysis: several positions by means of a grid of different latitudes and longitudes – steps of 5° in latitude and 10° in longitude – with the higher endpoints at specific height – 23222km corresponding to the GALILEO constellation; three seasons – winter (December), equinox (March) and summer (June); three solar activity levels – low (Φ_{12}=63), mid (Φ_{12}=123) and high (Φ_{12}=183); and several times-of-day – two hours (0 and 12 UT) for maps and a set of hours (0 to 23 with step 1) for differences.

sTEC error analysis: different positions – all available stations and satellites at 20200km for the GPS constellation; two seasons – winter (January) and summer (July); two periods in the 11-year solar cycle – peak in 2000 and mid in 2004; different times-of-day – all available hours from 0 to 23.9 as the last measurement should be 10 minutes before midnight; and different days without geomagnetic storms (*Kp* index < 5).

Table 1. Statistical characterization of differences in vTEC and sTEC analysis

	Absolute	Relative
Bias	$\left\langle TEC_{ref} - TEC_{mod} \right\rangle$	$\left\langle \frac{TEC_{ref} - TEC_{mod}}{TEC_{ref}} \right\rangle$
Maximum	$\max\left(TEC_{ref} - TEC_{mod}\right)$	$\max\left(\frac{TEC_{ref} - TEC_{mod}}{TEC_{ref}}\right)$
RMS	$\left\langle \left(TEC_{ref} - TEC_{mod}\right)^2 \right\rangle$	$\left\langle \left(\frac{TEC_{ref} - TEC_{mod}}{TEC_{ref}}\right)^2 \right\rangle$

Profile analysis

These tests allow to understand the consequences of the proposed modifications and developments. Fig. 7 presents profiles for the different developments for ESTEC location in the month of March, Φ_{12}=123 and at 13h UT. Fig. 7.a shows the ITU-R baseline. In Fig. 7.b, unrealistic peculiarities in the height profiles are avoided thanks to simplifications from NeQuick developments (2002). In this case, the modification of the *k* parameter from NeQuick developments (2005a) implies a denser topside (see Fig. 7.c) which can reveal itself as problematic for equatorial regions as the modelled ionosphere is already too dense for these regions. NeQuick developments (2005b) bring a "big" modification in the sense that the most important feature (anchor point F_2 layer peak) changes (see Fig. 7.d). With its less dense topside in Fig. 7.e, an interesting compromise with Fig. 7.c seems possible from NeQuick 2006b. Finally Fig. 7.f includes all modifications and shows the compromise reached for the topside.

vTEC analysis

For the analysis of differences on a global scale, vTEC grid maps have been used. As a consequence, the global evolution is characterized to establish whether the modifications have beneficial consequences such as a weaker latitudinal dependence of NeQuick error considering only ITU-R version and NeQuick developments (2005b) and (2006).

Fig. 8 presents global vTEC maps generated on a grid of 5° in latitude and 10° in longitude, for a day in March, with Φ_{12}=123 and at 12h UT. For the ITU-R (see Fig. 8a) version, a maximum value of 82 TECu is found close to the equatorial anomaly. Fig. 8.b shows NeQuick developments (2005b) a maximum value of 65 TECu, which seems to reduce the known average mismodelling of NeQuick overestimating TEC on equatorial areas. The maximum value for NeQuick developments (2006) is even lower and equal to 58 TECu (see Fig. 8.c). However, the overall shape of the map did not change so that the differences can represent only an offset due to its simplicity.

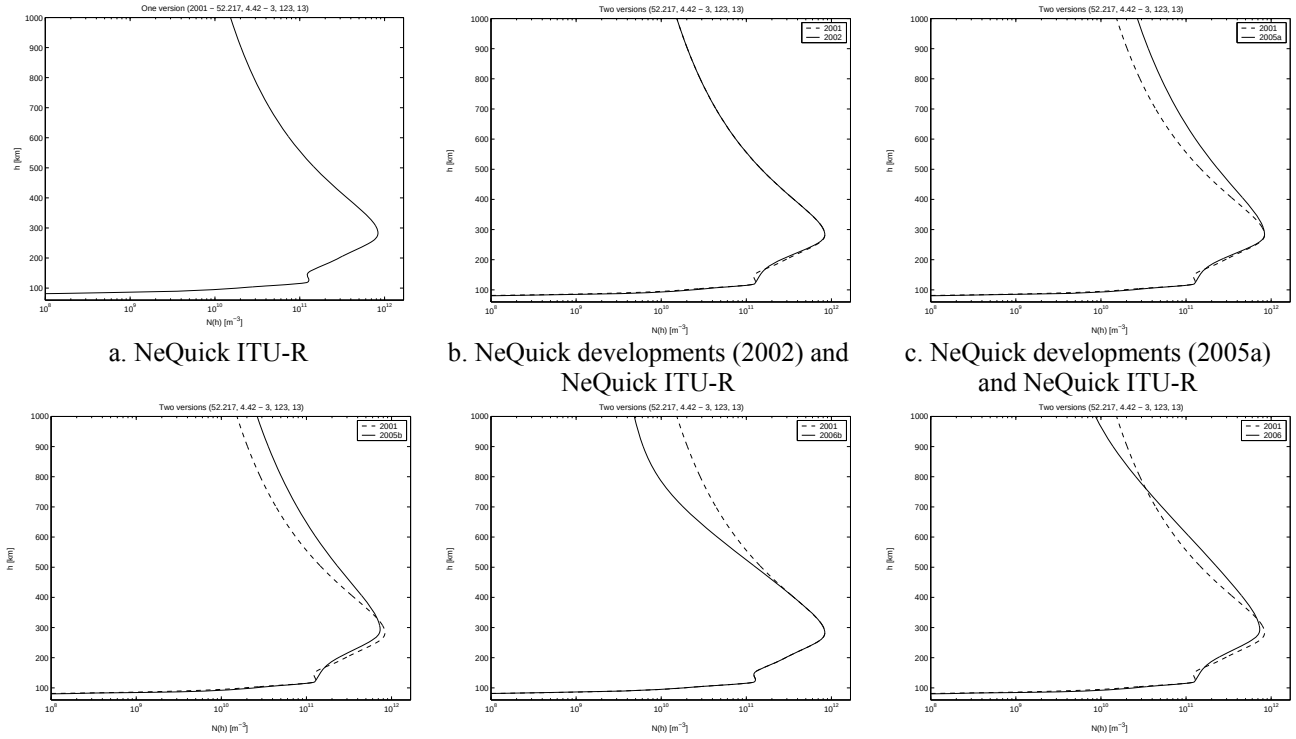

a. NeQuick ITU-R

b. NeQuick developments (2002) and NeQuick ITU-R

c. NeQuick developments (2005a) and NeQuick ITU-R

d. NeQuick developments (2005b) and NeQuick ITU-R

e. NeQuick developments (2006b) and NeQuick ITU-R

f. NeQuick developments (2006) and NeQuick ITU-R

Fig. 7. Electron density profiles comparisons (reference curve NeQuick ITU dashed)

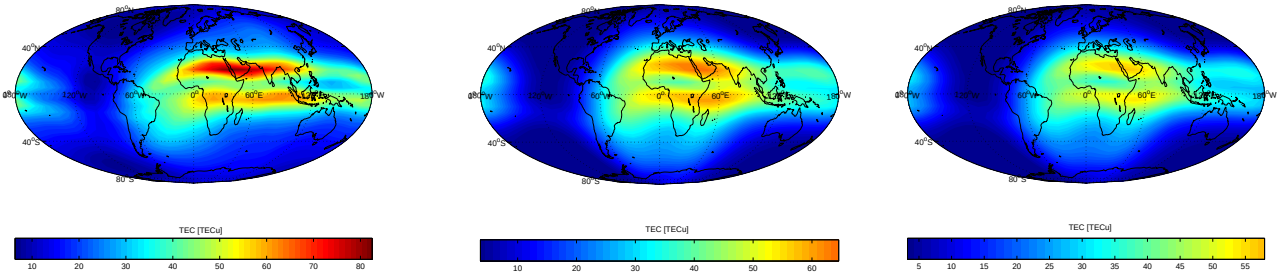

a. NeQuick 2001 (version 1, ITU-R) b. NeQuick developments (2005b) c. NeQuick developments (2006)

Fig. 8. vTEC maps

sTEC analysis

Table 2 presents the sTEC analysis for sTEC data from 45 IGS stations generated with the method explained in [21], for all visible satellites, during 5 days of the month of January 2000, from 00:30 to 23:30 UT. An elevation mask of 30 degrees was applied to the data since for some stations, a few low elevation sTEC values were unrealistically low. The input Φ_{12} is the monthly smoothed value obtained for that month from the SIDC database. The negative bias of NeQuick ITU-R highlights a general tendency of average overestimation of the TEC values which decreases for the newer NeQuick versions, however, the RMS value is slightly lower for the ITU-R version. NeQuick developments (2006) show the lowest bias but the largest RMS.

This analysis is not conclusive on an absolute sense since the sTEC dataset can also present a bias with respect to reality which has not been considered. Furthermore, a monthly smoothed value of the flux was used for NeQuick, which can present very large day-to-day variations in the performance of the model. However, this kind of analysis opens a path on a possible way to verify the performance of new developments of NeQuick. A more general sTEC analysis in the frame of GALILEO ionospheric single frequency algorithm is presented in [8].

5. CONCLUSIONS AND FUTURE WORK

As intended, the paper have provided a structured basis for future improvements of NeQuick, including

- a better understanding of the model,
- a number of problems that need to be addressed,
- analysis tools allowing to visualize the evolution of the model constitutive parameters and results,
- and, preliminary tests demonstrating the procedure to characterize potential improvements.

As it was already highlighted, a new version of NeQuick including some of the developments explained in the paper should bring some improvements on the performance as its error behaviour towards latitude shows a better agreement with reality. It should be coupled to a less simplistic topside formulation involving several layers with appropriate transitions like the proposal named NeQuick developments (2006).

The paper contains a good description of the main components of the NeQuick model, its evolutions and most of its relevant references being a good starting point for those researchers planning to work with NeQuick in the future.

This study opens a number of possibilities for potential improvements that needs to be continued:

- a broader "physical" behaviour analysis,
- topside formulations research,
- intrinsic modification considerations for daily use,
- and finally an "effective" use analysis.

Table 2. sTEC analysis

	NeQuick ITU-R	NeQuick developments (2005b)	NeQuick developments (2006)
Bias (TECu)	-1.58	2.88	0.25
RMS (TECu)	8.24	9.80	10.00

7. ACKNOWLEDGEMENTS

The work presented in this paper was part of B. Bidaine's Master Thesis [18]. For him, this work was the occasion to be involved in a team working in an highly skilled international environment, getting in touch with various actors from the field. Benoit would like to acknowledge Roberto Prieto-Cerdeira, Antonio Martellucci, Bertram Arbesser-Rastburg and the Sections of Wave Interaction and Propagation (TEC-EEP) and Antennas (TEC-EEA), in ESTEC; Sandro Radicella, Pierdavide Coïsson and Bruno Nava from ARPL in Trieste as well as René Warnant from RMI in Brussels. He is also grateful to the Belgian National Fund for Scientific Research (FNRS) for its financial support received to attend NAVITEC'2006.

APPENDIX 1. NEQUICK ITU-R VERSION

Bottom side

NeQuick bottom side is based on the Di Giovanni and Radicella (DGR) approach which proposed a method based on Epstein layers to calculate the electron density in the ionosphere ([21],[23]). This so-called DGR "profiler" concept uses the peaks of the E, F_1 and F_2 layers as anchor points.

The DGR models show a common bottom side description: up to the F_2-layer peak. They consist of a sum of Epstein layers [21]. The shape of an Epstein layer representing the electron density $N(h)$ [10^{11}.electrons.m^{-3}] is given by the following expression [24]:

$$N(h) = 4\, N_{\max} \frac{\exp\left(\frac{h - h_{\max}}{B}\right)}{\left(1 + \exp\left(\frac{h - h_{\max}}{B}\right)\right)^2} \tag{4}$$

where $N_{\max}$ [10^{11}.electrons.m^{-3}] denotes the peak amplitude, $h_{\max}$ [km] is the height of the peak and B [km] is the thickness parameter.

To model the electron density of ionosphere, the best agreement was found by dividing each layer L (where L can be E, F_1 or F_2), with corresponding peak characteristics $N^L_{\max}$ and $h^L_{\max}$, into its lower and its upper part by using two different thickness parameters, respectively B^L_{bot} and B^L_{top} [25]. Depending on the current height, bottom or top layers are chosen and the electron density results from the sum of the three components as follows:

$$\begin{aligned} N(h) &= \sum_L N^L(h) \\ &= \sum_L 4\, N^L_{\max} \frac{\exp\left(\frac{h - h^L_{\max}}{B^L}\right)}{\left(1 + \exp\left(\frac{h - h^L_{\max}}{B^L}\right)\right)^2} \end{aligned} \tag{5}$$

Fig. 9 shows the shape of the five components and their sum for characteristic values of the parameters in Table 3.

Table 3. Epstein parameters corresponding to Fig. 9

	E	F_1	F_2
$N^L_{\max}$ [10^{11} $el.m^{-3}$]	1.23	1.42	4.2
$h^L_{\max}$ [km]	120	195	263
B^L_{bot} [km]	5	15.8	29
B^L_{top} [km]	11.3	22.6	

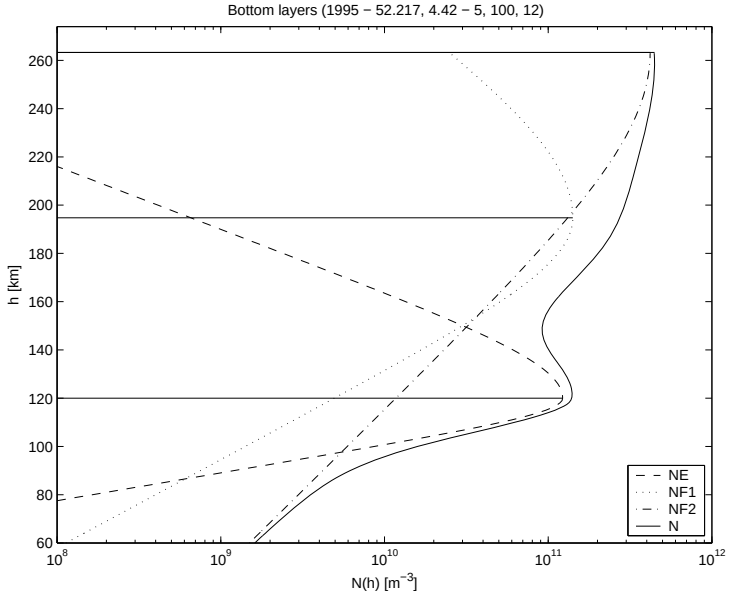

Fig. 9. Bottom side profile example (ESTEC location – 52.217°N, 4.42°E –, May, average solar flux – Φ_{12}=100–, midday universal time)

The Epstein parameters introduced in the previous subsection can be considered as intermediate values between the final profile and the input data based on measurements i.e. the ionosonde parameters, the critical frequencies f_0L and the transmission factor $M(3000)F_2$.

1. The peak amplitudes $N^L{}_{\max}$ are derived from the global electron densities at the peak height of layer L (NmL) [25], neglecting the E layer when considering the F_1 and F_2 layers, and assuming the amplitude of the F_1 layer at the F_2 peak:

$$\begin{aligned} N^E_{\max} &= N(h^E_{\max}) - N^{F_1}(h^E_{\max}) - N^{F_2}(h^E_{\max}) \\ &= NmE - N^{F_1}(h^E_{\max}) - N^{F_2}(h^E_{\max}) \end{aligned} \tag{6}$$

$$\begin{aligned} N^{F_1}_{\max} &= N(h^{F_1}_{\max}) - N^{E}(h^{F_1}_{\max}) - N^{F_2}(h^{F_1}_{\max}) \\ &= NmF_1 - N^{F_2}(h^{F_1}_{\max}) \end{aligned} \tag{7}$$

$$\begin{aligned} N^{F_2}_{\max} &= N(h^{F_2}_{\max}) - N^{E}(h^{F_2}_{\max}) - N^{F_1}(h^{F_2}_{\max}) \\ &= NmF_2 - N^{F_1}(h^{F_2}_{\max}) \\ &= NmF_2 - 0.1\,NmF_1 \end{aligned} \tag{8}$$

   NmL is calculated from the critical frequencies f_0L as [1]:

$$NmL = 0.124\, f_0 L^2 \tag{9}$$

2. The peak heights are defined through more complicated empirical equations [25] apart from $h^E{}_{\max}$ which is fixed at 120km. $h^{F1}{}_{\max}$ depends on NmF_1 and the magnetic dip (I) [26], whereas $h^{F2}{}_{\max}$ is described by means of the ratio f_0F_2/f_0E and the transmission factor $M(3000)F_2$ [27].

3. Finally the main *thickness parameters* are $B^{F2}{}_{\text{bot}}$ and $B^{F1}{}_{\text{top}}$ as the others are based on the latter or fixed at a certain value [25]. $B^{F2}{}_{\text{bot}}$ is calculated from NmF_2 and the gradient of $N(h)$, $(\mathrm{d}N/\mathrm{d}h)_{\max}$, at the characteristic point in the base of the F_2 layer, i.e. the first derivative of (4) for F_2 layer at the inflection point. $B^{F1}{}_{\text{top}}$ is obtained from (4) and the same assumption as in (8).

Table 3 gives an example of the values of the Epstein parameters and lets guess the relation between $B^{F1}{}_{top}$ and $B^{F1}{}_{top}$ (multiply by 0.7), $B^{F1}{}_{top}$ and $B^{E}{}_{top}$ (half when F_1 is present) and the constant value of $B^{E}{}_{bot}$ (5km). Table 4 contains the ionosonde parameters corresponding to the example in Fig. 9. They represent the general variations of the ionosphere described through so-called "maps", i.e. their values are calculated on the basis of measured data – from vertical incidence soundings at a certain number of ground stations all over the world – by means of empirical equations. The most common maps allow computing monthly medians, describing well the evolution during a day but showing no difference from day to day during the same month.

1. f_0E and f_0F_1 appear to be closely correlated so that, in the ionospheric model used in this study, f_0F_1 is calculated from f_0E ([28],[29]). They depend in general:
   - on solar activity through the monthly solar radio flux at a wavelength of 10.7cm, Φ [10^{-22}Wm^{-2}Hz^{-1}];
   - and, on position, season and time-of-day through the cosine of the zenith angle of the Sun, χ [degrees].
2. The treatment of f_0F_2 and $M(3000)F_2$, which are related to the main ionospheric layer F_2, is more complex regarding their more complicated variations towards time and latitude [30]. They are generated by means of numerical maps
   - based on monthly sets of coefficients defining the map – the most common sets were released by the CCIR (Consultative Committee for International Radio) in 1967 and define the so-called "CCIR maps" ;
   - and consisting in a Fourier time series [31] where two big influences – from the Sun and the geomagnetic field – can be highlighted through the use of two particular variables: the monthly smoothed sunspot number R_{12} (10) or the equivalent monthly smoothed solar flux Φ_{12} (11) [32] and the Modified Dip latitude (MODIP or μ) [degrees] (12) [30].

$$R_{12} = \frac{1}{12}\left[\frac{R_{n-6}}{2} + \sum_{k=n-5}^{n+5} R_k + \frac{R_{n+6}}{2} \right] \tag{10}$$

where R_k is the mean of the daily sunspot numbers for a single month k, and R_{12} is the smoothed index for the month represented by k=n.

$$\Phi_{12} = 63.7 + 0.728\ R_{12} + 8.9\ 10^{-4}\ R_{12}^2 \tag{11}$$

$$\tan\mu = \frac{I}{\sqrt{\cos\varphi}} \tag{12}$$

where I [degrees] denotes the magnetic dip and φ [degrees] is geographic latitude.

As mentioned above, the DGR approach using three Epstein layers – one for each ionospheric layer – was first proposed in [21]. It was later improved by dividing each layer into its top and bottom side leading to a bottom side formulation constituted of five, so-called semi-Epstein layers. Further improvements were proposed from two main modifications [33] comprising the formulation of NeQuick:

1. The lowest part (below 100 km) was replaced by the bottom side of a Chapman layer.

$$N(h) = N_0\ \exp\left(1 - b\,\frac{h-h_0}{H_0} - \exp\left(-\frac{h-h_0}{H_0}\right)\right)$$
$$b = 1 - \left[\frac{1}{N(h)}\frac{dN}{dh}(h)\right]_{h=h_0} \tag{13}$$

Where h_0=100 km, N_0 [10^{11}.electrons.m^{-3}], H_0=100 km.

Table 4. Ionosonde parameters and peak height electron densities corresponding to Fig. 9

	E	F_1	F_2	$M(3000)F_2$
$f_0L\,[MHz]$	3.35	4.69	6	2.94
$NmL\,[10^{11}\ el.m^{-3}]$	1.39	2.73	4.46	

2. A fading out effect was added to the E and F_1 layers in the vicinity of the F_2 layer peak to ensure that the electron density at the F_2 layer peak corresponds exactly to f_0F_2 providing the direct calculation of $N^{F2}{}_{\max}$ from f_0F_2 by means of (9). Equation (8) is then replaced by:

$$N_{\max}^{F_2} = 0.124\, f_0 F_2^{\,2} \tag{14}$$

To implement this effect, the arguments of the exponential functions corresponding to E and F_1 in (6) were multiplied by a coefficient ζ:

$$\zeta(h) \;=\; \exp\left(10 \big/ (1 + 2\,|\,h - h_{\max}^{F_2}\,|)\right)$$

Fig. 10 shows the resulting profile for the same conditions as Fig. 9 but up to 1000 km height. In [11], it is explained this overall evolution and extends it to the topside which allows to differentiate NeQuick to other models of the DGR family.

Topside

The simplest way to take the topside into account is to consider it as a sixth semi-Epstein. However, it received a different thickness parameter which evolved from the beginning, even before constituting the difference between the three models of the DGR family.
The first idea was to *adapt* modelled TEC values to measurements ([11],[25]) using an additional parameter k for the top F_2 layer, considering only this layer and getting back to the meaning of the thickness parameter B.

$$\begin{aligned} TEC &= TEC_{bot} + TEC_{top} = 2\, N_{\max}^{F_2}\; B_{bot}^{F_2} + 2\, N_{\max}^{F_2}\; B_{top}^{F_2} \\ &= 2\, N_{\max}^{F_2}\; B_{bot}^{F_2}\, (1+k) \end{aligned} \tag{15}$$

The thickness parameter was then given by the equation $B^{F2}{}_{\text{top}} = k.B^{F2}{}_{\text{bot}}$ where k could range from 2 to 8.
An even better agreement was found in [11] using a coefficient υ and replacing $B^{F2}{}_{\text{top}}$ by a new height dependent thickness parameter H [15] reaching the current form of the profile which is shown in Fig. 10 with $B^{F2}{}_{\text{top}}$ =46.2 km.

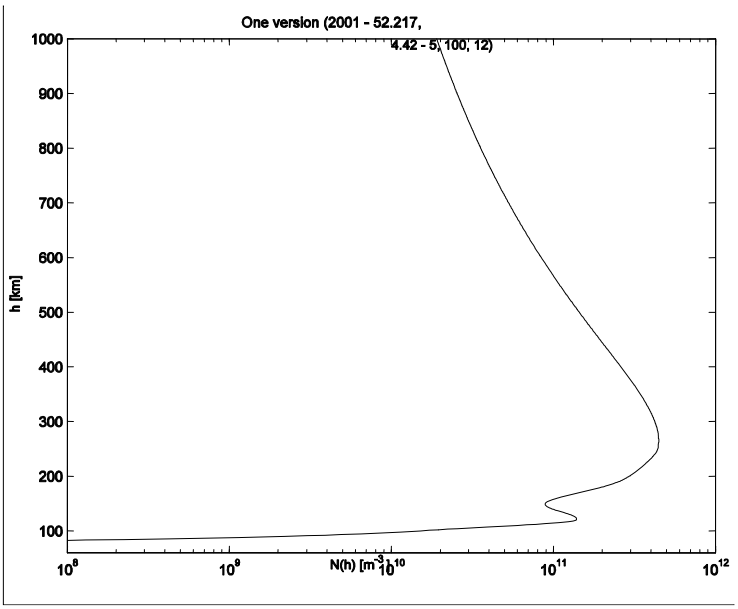

Fig. 10. Profile up to 1000 km example from NeQuick version 1 (ITU-R) (ESTEC location – 52.217°N, 4.42°E –, May, average solar flux – Φ_{12}=100–, midday universal time)

REFERENCES

[1] Davies, K., *Ionospheric Radio*, Peter Peregrinus , 1990.

[2] Goodman J. M. and Aarons J.,1990 "Ionospheric effects on modern electronic systems", *Proc. IEEE* Vol. 78 No. 3, 1990

[3] Flock, W.L., *Propagation Effects on Satellite Systems at Frequencies Below 10 GHz, A Handbook for Satellite Systems Design*, NASA Reference Publication 1108(02), Washington, D.C, 1987.

[4] Klobuchar, J., "Ionospheric effects on GPS," in *Global Positioning System: Theory and Applications*, Parkinson, Spilker, Axelrad, and Enge, Ed. Washington, DC: American Institute of Aeronautics and Astronautics, 1996.

[5] Kintner, P.M., Ledvina, B.M., "The ionosphere, radio navigation and global navigation satellite systems", *Advances in Space Research*, Volume 35, Issue 5, p. 788-811, 2005.

[6] Cander, L., Leitinger, R., and Levy M., "Ionospheric models including the auroral environment", in *ESA Workshop on Space Weather*, ESTEC, Noordwijk, The Netherlands, 11-13 November 1998.

[7] Klobuchar, J.A, "Ionospheric time-delay algorithm for single-frequency GPS users", *IEEE Trans. Aerospace and Electr. Syst. 1987*, AES-23: pp 325-331, 1987.

[8] Prieto-Cerdeira, R., Orus, R., Arbesser-Rastburg, B., "Assessment of the Ionospheric correction algorithm for GALILEO Single Frequency Receivers". In *Proceedings of the 3rd ESA Workshop on Satellite Navigation User Equipment Technologies NAVITEC 2006*, Noordwijk, The Netherlands, December 2006.

[9] ITU-R. "Ionospheric propagation data and prediction methods required for the design of satellite services and systems". Rec. ITU-R P.531-8, 2005.

[10] ITU-R NeQuick Software for ITU-R Rec. P 531-8, 2002 [Online]. Available: http://www.itu.int/ITU-R/study-groups/software/rsg3-p531-electron-density.zip

[11] Radicella, S. M., Leitinger, R. "The evolution of the DGR approach to model electron density profiles". *Adv. Space Res.*, Vol. 27, No. 1, p. 35-40, 2001.

[12] The 10th Generation International Geomagnetic Reference Field, [Online], Available: http://www.ngdc.noaa.gov/IAGA/vmod/igrf.html

[13] Corrected Geomagnetic Coordinates, [Online], Available: http://modelweb.gsfc.nasa.gov/models/cgm/cgmm_des.html

[14] Fonda, C., Coïsson, P., Nava, B. et al. "Comparison of analytical functions used to describe topside electron density profiles with satellite data". *Ann. Geophys.*, Vol. 48, No. 3, p. 491-495, 2005.

[15] Leitinger, R., Zhang, M.-L., Radicella, S. M. "An improved bottomside for the ionospheric electron density model NeQuick". *Ann. Geophys.*, Vol. 48, No. 3, p. 525-534, 2005.

[16] Coïsson, P., Radicella, S. M., Nava, B. "Tests of NeQuick with modified topside formulation". presented at 11th SBAS-IONO meeting, Noordwijk, 2005.

[17] Leitinger, R. *Personal communication*, 2005.

[18] Bidaine, B. "Ionosphere Crossing of GALILEO Signals". M.S. thesis. Liège: ULg (FSA), 2006.

[19] Jakowski, N., Kutiev, I. S., Heise, S. et al. "A topside ionosphere/plasmasphere model for operational applications". In *Proceedings of the XXVIIth URSI General Assembly*, Maastricht. p. 2174-2177, 2002.

[20] Knezevich, M., Radicella, S. M. "Development of an ionospheric NeQuick model algorithm for GNSS receivers". In *Proceedings of the 2nd ESA Workshop on Satellite Navigation User Equipment Technologies NAVITEC 2004*, Noordwijk, The Netherlands, December 2004.

[21] Ciraolo, L., Azpilicueta, F., Brunini, C., Meza, A., Radicella, S. M., "Calibration errors on experimental slant total electron content (TEC) determined with GPS", *Journal of Geodesy,* Online Article, September 2006.

[22] Di Giovanni, G., Radicella, S. M. "An analytical model of the electron density profile in the ionosphere". *Adv. Space Res.*, Vol. 10, No. 11, p. 27-30, 1990.

[23] Hochegger, G., Nava, B., Radicella, S. M. et al. "A Family of Ionospheric Models for Different Uses". *Phys. Chem. Earth (C)*, Vol. 25, No. 4, p. 307-310, 2000.

[24] Rawer, K. "Replacement of the present sub-peak plasma density profile by a unique expression". *Adv. Space Res.*, Vol. 2, No. 10, p. 183-190, 1983.

[25] Radicella, S. M., Zhang, M.-L. "The improved DGR analytical model of electron density height profile and total electron content in the ionosphere". *Ann. Geofis*, Vol. XXXVIII, No. 1, p. 35-41, 1995.

[26] Mosert de Gonzalez, M., Radicella, S. M. "An empirical model of the F_1 intermediate layer true-height characteristics". *Adv. Space Res.*, Vol. 7, No. 6, p. 65-68, 1987.

[27] Bradley, P. A., Dudeney, J. R. "A simple model of the vertical distribution of electron concentration in the ionosphere". *J. Atmos. Terr. Phys.*, Vol. 35, p. 2131-2146, 1973.

[28] Leitinger, R., Radicella, S.M., Nava, B. et al. "NeQuick – COSTprof - NeUoG-plas, a family of 3D electron density models". In *Proceedings of the COST 251 Madeira Workshop*, Madeira. p. 75-89, 1999.
[29] Leitinger, R., Titheridge, J. E., Kirchengast, G. et al. "Ein “einfaches” globales empirisches Modell für die F-Schicht der Ionosphäre" ["A "simple" global empirical model for the F layer of the ionosphere"]. *Kleinheubacher Ber.*, Vol. 39, p. 697-704, 1996.
[30] Rawer, K. "Propagation of Decameter Waves (HF-Band)". In Landmark, B. Ed. *Meteorological and Astronomical Influences on Radio Wave Propagation*. New York: Academic Press, Chap. 11, p. 221-250, 1963.
[31] ITU-R. "Reference ionospheric characteristics". Rec. ITU-R P.1239, 1997.
[32] ITU-R. "Choice of indices for long-term ionospheric predictions". Rec. ITUR P.371-8, 1999.
[33] Leitinger, R., Radicella, S.M., Nava, B. et al. "NeQuick – COSTprof - NeUoG-plas, a family of 3D electron density models". In *Proceedings of the COST 251 Madeira Workshop*, Madeira. p. 75-89, 1999.